Tunable elastic stiffness with microconfined magnetorheological domains at low magnetic field

Carmel Majidi[a] and Robert J. Wood
School of Engineering and Applied Sciences (SEAS), Harvard University, Cambridge, Massachusetts 02138, USA

(Received 28 June 2010; accepted 29 September 2010; published online 21 October 2010)

Surface micropatterning enhances the interfacial sliding resistance of magnetorheological fluid at low magnetic field (10–35 mT). Fluid is confined to surface microchannels, resulting in the formation of spatially aligned magnetic domains. The channels are supported by a pair of overlapping ribbons, which, along with the surrounding fluid, are enclosed in a soft elastomer. The embedded elastomer represents an electromagnetic alternative to current methods of active stiffness control that are based on principles of gel hydration, particle jamming, and pneumatics. © *2010 American Institute of Physics*. [doi:10.1063/1.3503969]

Actively controlling material impedance is enabling for emerging fields such as soft robots for exploration and natural disaster relief[1,2] and soft active orthotics for motor therapy and gait correction.[3,4] Recent efforts have focused on jamming techniques[5,6] such as pneumatic-controlled packing of granular particles in an elastomer-sealed chamber[2] and the hydration of a soft nanowhisker-gel composite, which solidifies when dry by forming rigid, cellulose networks.[7,8] Compliance control has also been accomplished with mechanisms that utilize, gears, pulleys, motors, and springs.[9,10] Designs have been inspired by a variety of systems in nature, including catch connective tissue in sea cucumbers[7,8] and muscular cocontraction in human motor tasks.[9,10]

Methods based on fluidic jamming and springs require the added complexity of external pumps, tanks, and motors and, hence, may not be suitable in low power or millimeter scale systems. One promising alternative is to use magnetorheological (MR) fluid, which solidifies in the presence of a strong magnetic field. Increasingly used in automotives and aerospace, MR-fluid has also been utilized for stiffness and damping control in adaptive orthotic devices.[11–15] However, solidification requires a large, 0.5–1 T magnetic field, which is prohibitive for small or low power devices. For these systems, adaptive functionality is aided by nonsolidfication modes of MR impedance control.

In this letter, we demonstrate reversible mechanical impedence with MR fluid at fields of 10–35 mT. This is accomplished by patterning the bounding surfaces with an array of microchannels. When a magnetic field is applied, the fluid in the channels form confined magnetic domains that resist separation as the overlapping surfaces slide past each other. As illustrated in Fig. 1(a), the microchannels are patterned on the inside surfaces of two overlapping ribbons. The ribbons and surrounding MR-fluid are enclosed in an ultrasoft polyurethane elastomer (Sorbothane®, elastic modulus ~1 MPa). The 1 cm wide, 1 mm thick plastic ribbons have an elastic modulus of 2 GPa (Veroblack, Objet Geometries Inc.) and are molded in a three-dimensional printer (Connex500™, Objet Geometries Inc.). Within the 5 cm long region of overlap, the ribbon surfaces contain channels that are 500 μm wide, 500 μm deep, and spaced 250 μm apart, as shown in Fig. 1(b). The ribbons are enclosed in a polyurethane-sealed chamber (Sorbothane®, 0030 Shore Hardness, 1 mm wall thickness) filled with MR fluid (MRF-140CG, LORD Corporation, solids content by weight =85.4%).

The MR fluid is composed of 5–10 μm diameter iron carbonyl (composition >99% Fe) microparticles that are randomly dispersed in a carrier oil. In the absence of a magnetic field, the only resistance to stretching is the intrinsic elastic stiffness of the elastomer and the viscous drag of the fluid inside the ribbon interface, which is illustrated in Fig. 1(c). Applying a magnetic field along the central axis of the ribbon (and perpendicular to the channel orientation) magne-

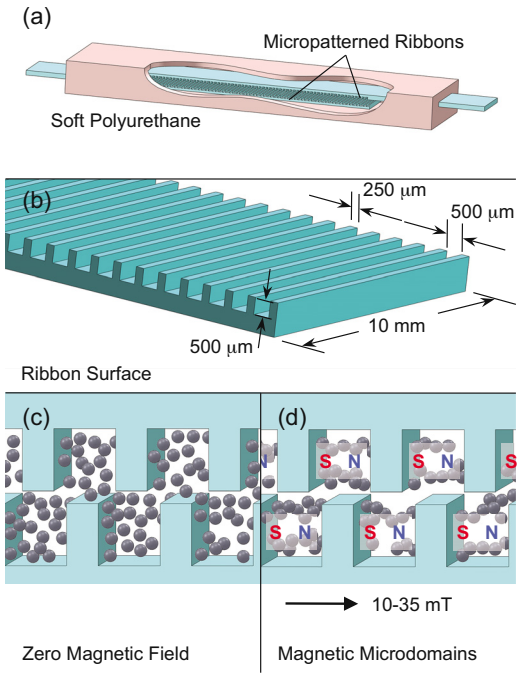

FIG. 1. (Color online) (a) An ultrasoft polyurethane elastomer is embedded with rigid, micropatterned ribbons that slide past each other. The tabs are enclosed in a chamber filled with MR fluid. (b) The surface of each ribbon is patterned with an array of aligned microchannels. (c) In the absence of magnetic field, the MR microparticles are randomly dispersed. (d) Under an external field of 10–35 mT, the microparticles form magnetic domains that are confined to the microchannels.

[a]Electronic mail: cmajidi@seas.harvard.edu.

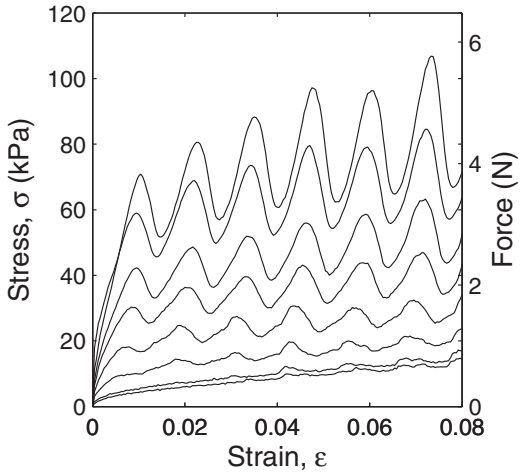

FIG. 2. Tensile strain vs stress for an applied magnetic field of (from bottom) 0, 5, 10, 15, 20, 25, 30, and 35 mT. The periodic fluctuations in tensile stress correspond to the surface microstructure, which is illustrated in Fig. 1(b), where the channels are 500 μm wide, 500 μm deep, spaced 250 μm apart and are supported by a ribbon that is 500 μm thick and 1 cm wide. The fluid-filled chamber containing the overlapping ribbons is approximately 6 cm long and so one percent strain corresponds to 600 μm.

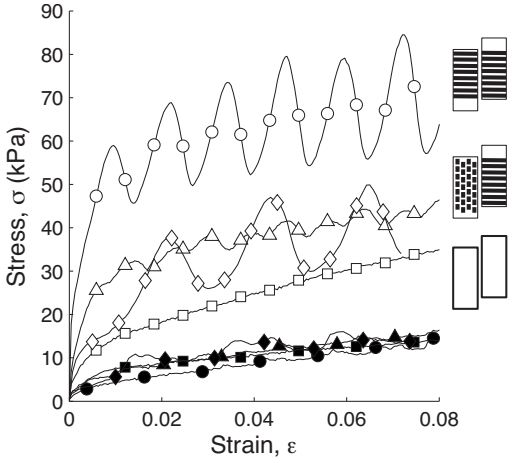

FIG. 3. Stress-strain curves for elastomers embedded with various ribbon surface geometries: (curve with circle markers) 500 μm wide channels, (square) smooth surfaces, (triangle) one surface contains staggered microgrooves, (diamond) 500 μm wide channels supported by a 3 cm long ribbon. Filled and open markers correspond to 0 and 30 mT of applied field, respectively.

tizes the particles and causes them to align and form magnetic domains within the channels of the opposing ribbons; see Fig. 1(d). Stretching the elastomer requires an enhanced friction force to separate the confined domains and slide the ribbons past one another.

A plot of strain versus tensile stress is presented in Fig. 2. The curves, from bottom to top, correspond to magnetic fields of 0, 5, 10, 15, 20, 25, 30, and 35 mT. Tensile tests were performed on a single column load cell (5544A Instron) at a speed of 15 mm/min. Past a strain of about one percent, the stress-strain curves exhibit periodic fluctuations with a period of 750 μm, equal to the center-to-center spacing of the surface channels. This is consistent with the postulate of confined magnetic domains, wherein the resistance to elastomer stretching fluctuates as magnetic bonds between the opposing channels are broken and then replaced with new bonds between newly aligned channels.

A comparison of strain-stress curves for various ribbon surface geometries are presented in Fig. 3. Curves with filled and open square markers correspond to 500 μm wide channels under an applied field of 0 mT and 30 mT, respectively. These same curves also appear in Fig. 2. Curves with filled and open square markers correspond to smooth, unpatterned ribbons under 0 mT and 30 mT, respectively. In the absence of magnetic field, both geometries exhibit similar stress-strain curves. In this regime, the mechanics are largely dominated by the elastic stretching of the polyurethane enclosure. However, under a field of 30 mT, the mechanical resistance of the unpatterned system is less than half of that of the system containing aligned, 500 μm wide channels.

As shown in the inset to Fig. 3, curves with triangular markers correspond to a pair of ribbons where one surface contains 750 μm wide channels that are spaced 250 μm apart while the opposing surface contains holes that are 750 μm long, 500 μm wide, and 500 μm deep. The curve under zero magnetic field (filled markers) is the same as for the unpatterned and 500 μm channel specimens. Under a field of 30 mT, the mechanical resistance (open markers) increases but is still half that of the elastomer containing the aligned 500 μm channels. Also, the curve does not exhibit significant periodic fluctuation. Together, these properties suggest that the staggered pattern neutralizes the alignment of magnetic poles across the interface and thus limits the mechanical resistance to stretching.

Lastly, the curves with diamond markers in Fig. 3 shows the stress-strain relationship for a pair of ribbons that overlap over 2.5 cm. The fluid-filled chamber has a total length 3.5 cm and so one percent strain corresponds to 350 μm of displacement. The ribbons are composed of 500 μm channels spaced 250 μm apart and so, as expected, a fluctuating stress-strain curve with 750 μm period is observed. Moreover, the mechanical resistance appears to be proportional to the length of the ribbon overlap. This is consistent with the magnetic domain model, which suggests that the force required to stretch the embedded elastomer and slide the interface is proportional to the number of interfacial magnetic bonds.

A theoretical estimate for the tensile resistance is derived by calculating the force between individual magnetic domains. For magnetic fields on the order of 10 mT, The MR fluid has a magnetic permeability μ of approximately 20 N/kA^2 (technical data for MRF-140CG, LORD Corporation). This corresponds to a relative permittivity of $\mu_r = \mu/\mu_0 = 16$ and a magnetic susceptibility of $\chi = \mu_r - 1 = 15$, where $\mu_0 = 1.256$ N/kA^2 is the vacuum permittivity. For an applied field of $B = 30$ mT, the fluid has a magnetization of $M = \chi B/\mu = 22$ kA/m.

The magnetized fluid is stored in parallel channels that slide past each other. Let x denote the distance between the centers of the channels in the direction of sliding. The total potential energy between channels is obtained by integrating the interaction energy of each pair across the interface, as follows:

$$U = \int_V \frac{\mu M^2}{4\pi r^3}\left\{\left(\frac{x_2 - x_1 + x}{r}\right)^2 - 1\right\} dV, \qquad (1)$$

where

$$r = \sqrt{(x_2 - x_1 + x)^2 + (y_2 - y_1 + D)^2 + (z_2 - z_1)^2},$$

$$\int_V = \int_{-L/2}^{L/2} \int_{-D/2}^{D/2} \int_{-w/2}^{w/2} \int_{-L/2}^{L/2} \int_{-D/2}^{D/2} \int_{-w/2}^{w/2},$$

$$dV = dx_1 dy_1 dz_1 dx_2 dy_2 dz_2.$$

Here, $L=1$ cm, $w=500$ μm, and $D=500$ μm are the length, width, and depth of the channels, respectively. According to the above equation, the sliding resistance $F=dU/dx$ reaches a maximum value of 12.7 mN when the centerlines of the channels are separated by a distance $x \approx 300$ μm along the direction of sliding. That is, F is greatest when the channels are roughly staggered such that the opposing magnetic poles are aligned. The surfaces of each overlapping ribbon contains 66 vertically aligned channels, and so the theory predicts that 0.84 N of force is necessary to shear the interface.

This theoretical analysis represents a simplified idealization of the interfacial mechanics. Referring to Fig. 2, the theoretical estimate of $F=0.84$ N is comparable to the experimentally measured amplitude of the oscillation under a field of 30 mT. However, it is several times smaller than the total difference in experimentally measured resistance between elastomers containing patterned and unpatterned ribbons. In order to obtain a more accurate theoretical estimate, it may be necessary to include fluidic and viscoplastic contributions into the analysis. The theory may also be improved by accounting for the mobility of the MR particles within the channels as well as the variation in magnetic susceptibility as the particles separate from the carrier oil.

In closing, a pair of micropatterned ribbons are immersed in an elastomer enclosed chamber of MR fluid. Applying magnetic field induces magnetic domains that are confined to the microchannels that line the overlapping surfaces. The force required to slide the ribbons past one another and stretch the elastomer scales with the number of channels and the intensity of the magnetic field. Experiments performed with various ribbon geometries suggest that the mechanics are governed by friction between channels of confined MR fluid. In addition to a refined theoretical analysis, future work should also focus on dynamical loading and hysteresis. Lastly, the principle of confined magnetic domains might be extended to the submicron scale with ferrofluids and nanopatterned surfaces.

The authors gratefully acknowledge support from the National Science Foundation (Award No. DMR-0820484). Any opinions, findings and conclusions or recommendations expressed in this material are those of the authors and do not necessarily reflect those of the National Science Foundation.

[1] S. Seok, C. D. Onal, R. J. Wood, D. Ru, and S. Kim, Proceedings of the IEEE International Conference Robotics and Automation, Anchorage, Alaska, 2010.
[2] E. Steltz, A. Mozeika, and H. Jaeger, Proceedings of the IEEE/RSJ International Conference Intelligent Robots and Systems, St. Louis, 2009.
[3] L. Stirling, C.-H. Yu, J. Miller, R. J. Wood, E. Goldfield, and R. Nagpal, Proceedings of the Shape Memory and Superelastic Technology Conference, Wyss Institute, Harvard University, Boston, MA, 2010.
[4] A. M. Dollar and H. Herr, Proceedings of the IEEE 10th International Conference Rehabilitation Robotics, Noordwijk, The Netherlands, 2007.
[5] M. E. Cates, J. P. Wittmer, J.-P. Bouchaud, and P. Claudin, Phys. Rev. Lett. **81**, 1841 (1998).
[6] V. Trappe, V. Prasad, L. Cipelletti, P. N. Segre, and D. A. Weitz, Nature (London) **411**, 772 (2001).
[7] J. R. Capadona, K. Shanmuganathan, D. J. Tyler, S. J. Rowan, and C. Weder, Science **319**, 1370 (2008).
[8] K. Shanmuganathan, J. R. Capadona, S. J. Rowan, and C. Weder, Prog. Polym. Sci. **35**, 212 (2010).
[9] G. A. Pratt and M. M. Williamson, Proceedings IEEE/RSJ Intelligent Conference Intelligent Robots and Systems, 1995, pp. 399–406.
[10] J. W. Hurst, J. E. Chestnutt, and A. A. Rizzi, Proceedings IEEE Intelligent Conference Robotics and Automation, New Orleans, LA, 2004.
[11] K. Koganezawa, Proceedings IEEE/RSJ Intelligent Conference Intelligent Robots and Systems, 2005, pp. 2512–2519.
[12] S. A. Migliore, E. A. Brown, and S. P. DeWeerth, Proceedings IEEE International Conference Robotics and Automation, Barcelona, Spain, 2005, pp. 4508–4513.
[13] H. Herr and A. Wilkenfeld, Ind. Robot **30**, 42 (2003).
[14] J. Z. Chen and W. H. Liao, Smart Mater. Struct. **19**, 035029 (2010).
[15] F. Ahmadkhanlou, J. L. Zite, and G. N. Washington, Proc. SPIE **6527**, 65270O (2007).